Absorption Studies of Neutral Retinal Schiff Base Chromophores

Iben B. Nielsen,[†] Michael Åxman Petersen,[‡] Lutz Lammich,[†] Mogens Brøndsted Nielsen,*[,‡] and Lars H. Andersen*[,†]

Department of Physics and Astronomy, University of Aarhus, DK-8000 Aarhus C, Denmark, and Department of Chemistry, University of Copenhagen, Universitetsparken 5, DK-2100 Copenhagen Ø, Denmark

Received: July 31, 2006; In Final Form: August 21, 2006

The neutral retinal Schiff base is connected to opsin in UV sensing pigments and in the blue-shifted meta-II signaling state of the rhodopsin photocycle. We have designed and synthesized two model systems for this neutral chromophore and have measured their gas-phase absorption spectra in the electrostatic storage ring ELISA with a photofragmentation technique. By comparison to the absorption spectrum of the protonated retinal Schiff base in vacuo, we found that the blue shift caused by deprotonation of the Schiff base is more than 200 nm. The absorption properties of the UV absorbing proteins are thus largely determined by the intrinsic properties of the chromophore. The effect of approaching a positive charge to the Schiff base was also studied, as well as the susceptibility of the protonated and unprotonated chromophores to experience spectral shifts in different solvents.

Introduction

Many biological species use retinylidene proteins, or opsins, for light energy conversion or to gain information about the surroundings, one example being bacteriorhodopsin (λ_{max} 568 nm) found in the membrane of halobacteria. Here, light absorption leads to proton pumping across the cell membrane, and the proton gradient thus formed is used for synthesizing ATP.[1] Other examples of opsin proteins are rhodopsin (λ_{max} 498 nm) and the visual pigments (λ_{max} 425 nm (blue), 530 nm (green), and 560 nm (red)) in human eyes enabling dim light and color vision, respectively. As a result of light absorption, large structural changes of the rhodopsins occur, and this leads to the triggering of an enzymatic signaling cascade, which finally creates a nerve impulse corresponding to the visual information.[2,3] The light sensor function is also encountered in the sensory rhodopsins of halobacteria. Sensory rhodopsin I (λ_{max} 587 nm) induces movement of the bacteria toward areas with solar light for efficient functioning of bacteriorhodopsin, while sensory rhodopsin II (λ_{max} 487 nm) makes the bacteria move away from areas with high energy blue or UV light and hence avoids oxidative photodamage.[1]

Despite the very different biological functions of opsin proteins, and despite the fact that they are found in as diverse species as humans and bacteria, the proteins share a very similar structure and features of their photocycle. They are all membrane proteins with seven trans-membrane α-helices,[4,5] and the chromophore is in all cases retinal,[2] in the all-trans form in the halobacterial opsins and in the 11-cis form in the rhodopsins. In both cases, the retinal is linked to the apoprotein via a Schiff base linkage to a specific lysine residue on the seventh helix.

Even though the Schiff base is protonated in the ground state in a large majority of the opsins, the neutral Schiff base is also encountered. One example is the intermediate produced in the photocycle of most opsin proteins. Light absorption triggers a very fast isomerization of the retinal chromophore (all-trans to 13-cis in the case of halobacterial proteins and 11-cis to all-trans in the case of rhodopsin).[6] The isomerization is followed by a proton transfer from the Schiff base to a nearby amino acid residue making the Schiff base neutral. In rhodopsin, this intermediate is known as metarhodopsin II (λ_{max} 380 nm) and functions by triggering the visual signaling cascade already mentioned.[2,3] The neutral Schiff base intermediate in bacteriorhodopsin is termed the M intermediate (λ_{max} 410 nm). This intermediate corresponds to the state where the proton is transferred to the outside of the membrane via a hydrogen bond channel. Later, a similar channel on the cytoplasmic side is opened, such that the Schiff base is reprotonated by a proton transferred from the interior of the cell.[7]

Another example of a neutral Schiff base is found in UV sensing pigments. Some animals use UV vision for food foraging, mating, and communication. In some cases, it is still debated how the UV vision is achieved,[8] while there are strong indications that a deprotonated Schiff base is responsible for the large blue shift of the absorption maximum in, for example, mouse UV (λ_{max} 359 nm)[9] and invertebrate UV pigments.[10]

Finally, an example of an unprotonated Schiff base has been found in mutants of rhodopsin and other opsin proteins. In wild-type rhodopsin, the glutamate at position 113 (bovine rhodopsin counting) functions as the Schiff base counterion.[11,12] If this glutamate is mutated to a glutamine, the positive charge on the Schiff base can no longer be stabilized by the carboxylate group, and the Schiff base is therefore deprotonated. Deprotonation results in a drastic blue shift of the absorption maximum to around 380 nm in the case of rhodopsin.

The above-mentioned opsins with unprotonated Schiff bases all absorb in the UV area, whereas the ground states of the halobacterial opsins and the visual pigments have maximum absorption wavelengths in the visible part of the spectrum. Here, we study the extreme blue shift inferred by deprotonation of the Schiff base by recording the gas-phase absorption spectra

* Authors to whom correspondence should be addressed. E-mail: mbn@kiku.dk (M.B.N.); lha@phys.au.dk (L.H.A.).
[†] University of Aarhus.
[‡] University of Copenhagen.

10.1021/jp064901r CCC: $33.50
Published on Web 10/31/2006

CHART 1: Model System for the Protonated Schiff Base Retinal

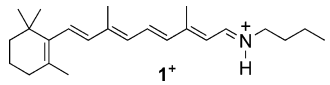

1$^+$

CHART 2: Model Systems for the Neutral Schiff Base Retinal

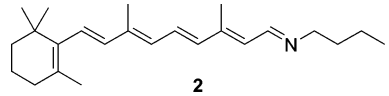

2

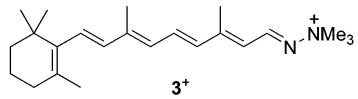

3$^+$

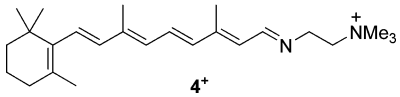

4$^+$

SCHEME 1

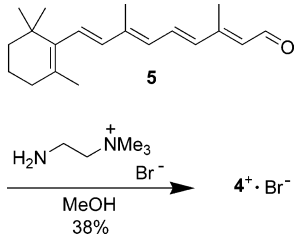

5

of neutral retinal Schiff bases. In the gas phase, the retinals are isolated from the protein thus avoiding external tuning effects imposed by the protein environment. Moreover, gas-phase spectra provide us with the possibility of studying solvation effects encountered in solutions by comparing the gas-phase spectra to spectra obtained in polar and unpolar solvents. One model of a neutral retinal Schiff base chromophore was previously synthesized, and the gas-phase absorption spectrum was measured in the electrostatic ion storage ring Aarhus (ELISA).[13] We now report a more thorough investigation including another neutral mimic. These data will be compared to previous studies on the protonated retinal Schiff bases (such as **1**$^+$)[13−15] in order of quantifying the spectral shift caused by deprotonation of the retinal Schiff base.

Design and Synthesis of Model Systems. Since it is not possible to study neutral molecules (e.g., **2**, Chart 2) with the storage ring technique, a charge needs to be added to the neutral retinal Schiff base but at a position where it is believed not to influence the absorption spectrum significantly, a so-called spectator charge. Two such retinals with neutral Schiff bases were designed with a $-N(CH_3)_3^+$ group as the spectator charge as seen in Chart 2. For the quaternized hydrazone **3**$^+$ studied in our previous work,[13] the $-N(CH_3)_3^+$ group is connected directly to the Schiff base, whereas two carbons separate the Schiff base and the spectator group nitrogen in **4**$^+$. For both model compounds, the charge is located outside the conjugated system of the chromophore.

The iodide salt of **3**$^+$ (**3**$^+$·I$^-$) was prepared according to a procedure by Dawson et al.,[16] while the bromide salt of **4**$^+$ (**4**$^+$·Br$^-$) was obtained in one step from all-*trans*-retinal **5** (Scheme 1) upon treatment with 2-aminoethyltrimethylammonium bromide at 5 °C.

Experimental Section

Gas-Phase Absorption Spectra. To measure the gas-phase absorption spectra, the chromophore models are transferred into the gas phase by use of an electrospray ion source,[17] seen in the inset of Figure 1. A methanol solution of the model chromophore is electrosprayed from a needle by applying a bias voltage of a few kilovolts. The solvent is then evaporated in a heated capillary, and the gas-phase ions are focused and steered through the ion source. To enhance the ion density, the ions are accumulated in a 22-pole ion trap, where helium gas removes excess energy from the ions. After 100-ms accumulation, the ions are extracted in a bunch containing about 10^4 ions and are accelerated to 22 kV. Finally, the desired ion mass is selected by a bending magnet, and the ion bunch is injected into the electrostatic storage ring (ELISA[18,19]), shown in Figure 1. Here, it circulates with a revolution time of around 75 μs.

After typically 50 ms of storage, the ion bunch is irradiated with a tunable nanosecond laser pulse in the upper straight section of ELISA. Absorption of photons increases the internal temperature of the ions,[20] and after some time it will eventually lead to dissociation provided that the energy is not radiated away. In this way, fragments, of which some will be neutral, are created. When neutral particles are formed by fragmentation (regardless of the process that causes the fragmentation), they will no longer be kept in orbit in the storage ring but will continue on straight trajectories. If the fragmentation takes place in the straight section opposite laser interaction, the neutral particles will impact on a microchannel plate detector situated at the exit of the ring. This signal is accumulated in channels corresponding to the time after injection, and the time evolution of neutral production may hence be followed. The excess production of neutral fragments caused by the laser pulse is clearly seen in the inset in Figure 1 on top of a small background caused by collisions with residual gas in the ring. Also seen is the large production of neutral fragments right after injection originating from hot ions produced, for example, during extraction from the trap.

The wavelength range to be covered for studying the chromophores is large, and therefore we have employed two different types of pulsed lasers. We used an alexandrite laser (PAL101, Light Age, Inc.) which is frequency doubled after the cavity. The second harmonic (361−397 nm) was either used directly or the frequency was shifted to the first Stokes or anti-Stokes lines in a Raman cell with D_2 (250 psi). With this method, wavelengths between 333 and 433 nm were produced. For wavelengths above 420 nm, an OPPO (optical parametric power oscillator, Lambda Physik) pumped with the third harmonic of a Nd:Yag laser (Infinity, Coherent) was used. The pulse energy (E_{pulse}) is measured with a power meter after the exit from the ring and is averaged over the data-acquisition time. The wavelength of the laser light (λ) is monitored with a fiber spectrometer.

To obtain the absorption profile (i.e., the absorption cross section), we first define the yield of neutral particles because of photon absorption. In a time window from the laser interaction time to the point where the neutral count rate is again reduced to the background level, all neutral counts are integrated giving $N_{signal}(\lambda)$ (the second black area seen in the inset in Figure 1). The average number of background counts (N_0) is determined by integrating the counts in a time window just before the laser interaction, (the first black area in Figure 1). N_0 is used to correct the signal ($N_{signal}(\lambda)$) for background counts. It is also used for normalization since it is proportional to the number of ions in

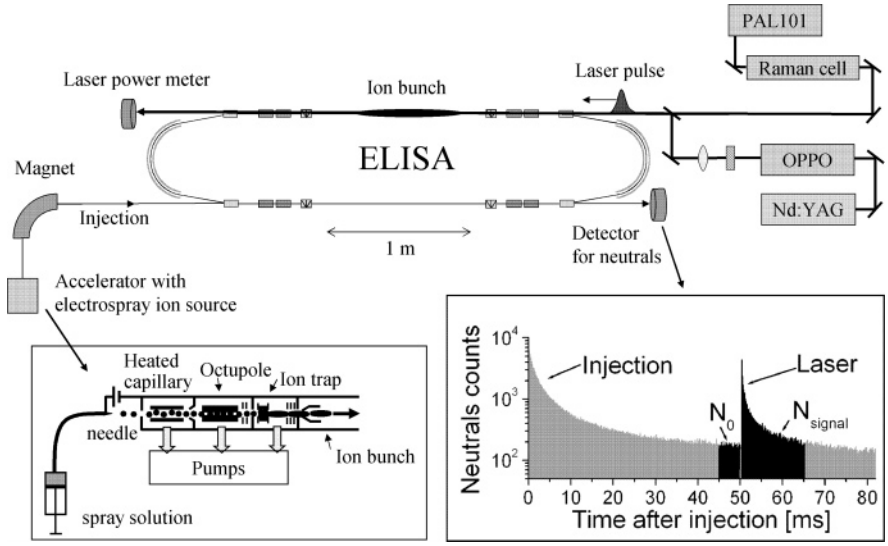

Figure 1. The electrostatic ion storage ring ELISA. The lower part of the ring is the injection and detection section, and the upper part is the laser interaction section. In the inset to the left, the electrospray ion source is seen. In the inset to the right, the counts of neutrals as a function of time is seen for the $\mathbf{3}^+$ chromophore at 510 nm. The windows used for calculation of the absorption cross section are indicated.

ELISA. We define the yield ($Y(\lambda)$) as

$$Y(\lambda) = \frac{N_{\text{signal}}(\lambda) - N_0}{N_0} \tag{1}$$

When calculating the absorption cross section, we assume that the quantum yield for photofragmentation is wavelength independent and that the overlap area between the ion bunch and the laser pulse remains constant. Furthermore, we assume a linear dependence of the yield on the number of photons in a pulse. Actually, saturation is observed at high-laser-pulse energies, but the error is minimized by keeping the average laser-pulse energy low and constant. Hence, we further normalize the yield to $E_{\text{pulse}}\cdot\lambda$, which is proportional to the number of photons in a pulse. The resulting formula for the relative absorption cross section (σ_{abs}) at a given wavelength is the following:

$$\sigma_{\text{abs}}(\lambda) = \frac{Y(\lambda)}{E_{\text{pulse}}\cdot\lambda} \tag{2}$$

Since the different laser sources have different beam profiles, the assumption of constant overlap between laser and ion beam is not necessarily fulfilled. There is not always an overlap in the wavelength range between the laser sources, and therefore individual parts of the spectrum may be scaled somewhat relative to each other. However, this does not significantly change the observed positions of the absorption maxima.

Solution Absorption Spectra. Absorption spectra of model chromophores in solution were recorded on a Cary50 (Varian Inc.) with pure solvent as baseline.

Synthesis of $\mathbf{4}^+\cdot\mathbf{Br}^-$. 2-Aminoethyltrimethylammonium bromide (40 mg, 0.22 mmol) was dissolved in dry MeOH (20 mL), whereupon all-*trans*-retinal **5** (50 mg, 0.18 mmol) and 4 Å molecular sieves were added. After stirring overnight at 5 °C, the reaction mixture was filtered and evaporated in vacuo, redissolved in CH_2Cl_2, filtered, and precipitated with *n*-pentane, which after filtration gave $\mathbf{4}^+\cdot Br^-$ (30 mg, 38%) as a red-brownish powder. δ_H/ppm (300 MHz, $CDCl_3$, 25 °C, 7.26 ppm) 8.44 (1 H, d, J = 10.5 Hz, C*H*=N), 6.87 (1 H, dd, J = 11.5 Hz, J = 15.0 Hz, C*H*), 6.31 (1 H, d, J = 15.1 Hz, C*H*), 6.24 (1 H, d, J = 17.6 Hz, C*H*), 6.09 (3 H, m, C*H*), 4.01 (4 H, m, NCH_2), 3.52 (9 H, s, NCH_3), 2.18 (3 H, s, CH_3), 1.97 (5 H, m, CH_2, CH_3), 1.72 (3 H, s, CH_3), 1.60 (2 H, m, CH_2), 1.47 (2 H, m, CH_2), 1.03 (6 H, s, CH_3); δ_C/ppm (75 MHz, $CDCl_3$, 25 °C, 77.0 ppm) 162.9, 147.0, 139.0, 137.6, 137.2, 135.2, 129.9, 129.7, 129.2, 128.4, 128.0, 66.9, 55.3, 54.6, 39.5, 34.2, 33.0, 28.9, 21.7, 19.1, 13.3, 12.8; *m*/*z* (HR−FAB$^+$, NBA) 369.3264 (M^+, $C_{25}H_{41}N_2$ requires 369.3270). [NMR spectra were recorded on a Varian instrument, using the residual solvent as the internal standard. Samples were prepared using $CDCl_3$ (Cambridge Isotope Labs) dried over molecular sieves (4 Å) and neutralized with basic Al_2O_3. Fast atom bombardment (FAB) mass spectra were obtained on a JEOL JMS-HX 110 Tandem Mass spectrometer in the positive ion mode using 3-nitrobenzyl alcohol (NBA) as matrix.]

Results and Discussion

In the gas phase, the protonated all-trans *n*-butyl retinal Schiff base $\mathbf{1}^+$ has its absorption maximum at 610 nm.[13] The two model chromophores with neutral Schiff bases both experience an immense blue shift compared to the protonated retinal Schiff base, as seen in Figure 2. The absorption maximum of $\mathbf{4}^+$ is at 388 nm, and the shift between the protonated ($\mathbf{1}^+$) and the unprotonated ($\mathbf{4}^+$) retinal Schiff bases is thus more than 200 nm! Compound $\mathbf{3}^+$ has its absorption maximum at 480 nm, which is between the maxima obtained for $\mathbf{1}^+$ and $\mathbf{4}^+$. All absorption data are collected in Table 1.

We clearly observe that the distance between the absorbing (chromophore) part of the molecule and the spectator charge has an influence on the position of the absorption maximum for the two neutral Schiff base models. From PM3 geometry optimizations employing the Gaussian program package,[21] we find distances between the Schiff base nitrogen and the spectator charge nitrogen of 1.50 Å for the $\mathbf{3}^+$ molecule and 2.98−3.71 Å (calculated from a variety of possible conformations) for the $\mathbf{4}^+$ molecule. The molecule with the spectator charge furthest away from the Schiff base ($\mathbf{4}^+$) hence has the absorption maximum furthest toward short wavelengths, since its spectator charge makes the smallest perturbation to the conjugated system. Indeed, the salt $\mathbf{4}^+\cdot Br^-$ experiences an absorption maximum at 368 nm in CH_2Cl_2, which is very close to that of the truly neutral retinal Schiff base **2** (λ_{max} 364 nm[22]). In contrast, the quaternized hydrazone salt $\mathbf{3}^+\cdot I^-$ exhibits a significantly red-shifted absorp-

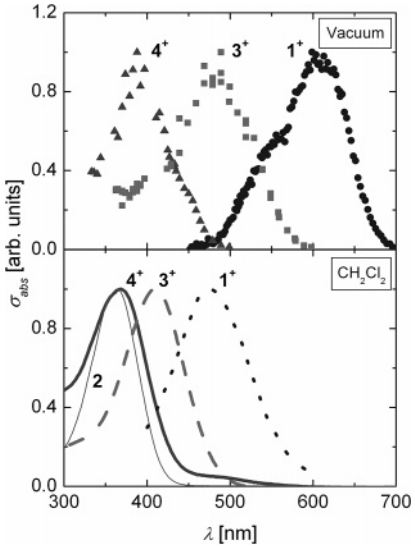

Figure 2. Upper part: Absorption spectra in the gas phase (left to right: $\mathbf{4}^+$ (triangles), $\mathbf{3}^+$ (squares), and $\mathbf{1}^+$ (circles)). Lower part: Absorption spectra in dichloromethane (left to right: $\mathbf{4}^+$ (thick line), **2** (thin line), $\mathbf{3}^+$ (dashed line), and $\mathbf{1}^+$ (dotted line)).

TABLE 1: Collection of Absorption Data

	$\mathbf{1}^+$	**2**	$\mathbf{3}^+$	$\mathbf{4}^+$
in vacuo	610		480	388
CH_2Cl_2	475	363 (364[a])	410	368
MeOH	445 (445[a])	364 (364[a])	389	

[a] Reference 22.

tion maximum in CH_2Cl_2 (λ_{max} 410 nm) relative to that of **2** (Figure 2). In other words, a positive charge in close proximity to the neutral Schiff base moves the absorption to longer wavelengths.

What is the origin of the almost 100-nm difference in absorption maxima of the two neutral Schiff base models $\mathbf{3}^+$ and $\mathbf{4}^+$? When retinal is excited from S_0 to S_1, a charge transfer from the β-ionone ring to the Schiff base is taking place,[23] that is, negative charge is transferred from the ring to the Schiff base. This negative charge transfer can qualitatively explain the shift between the two chromophores by considering what happens when the positive spectator charge is approaching the Schiff base (Figure 3).[24] With an almost even charge distribution, the S_0 state of the neutral chromophore is not disturbed much. The excited state will, on the other hand, be stabilized more in $\mathbf{3}^+$, where the spectator charge is closer to the Schiff base than in $\mathbf{4}^+$, resulting in an absorption spectrum of $\mathbf{3}^+$ which is shifted to the red compared to the spectrum of $\mathbf{4}^+$.

This interpretation is supported by a comparison of the solution spectra of $\mathbf{3}^+ \cdot I^-$ in CH_2Cl_2 and MeOH (Table 1). As MeOH is a more polar solvent, it is better able to solvate the positive charge of $\mathbf{3}^+$. The chromophore will hence be less perturbed by the spectator charge in MeOH than in CH_2Cl_2, and the absorption maximum is accordingly shifted in the direction of the true neutral chromophore from 410 to 389 nm. Naturally, hydrogen bonds, dipolar interactions, and the like may also be influential for the absorption shift between dichloromethane and methanol, but it may be noticed that there is no shift between the two solvents for **2**, and the solvation of the spectator charge by methanol is hence probably the most important factor.

Inspection of Figure 2 and Table 1 reveals that the absorption maxima of all the studied retinal chromophores are blue shifted upon solvation. The protonated retinal Schiff base ($\mathbf{1}^+$), however,

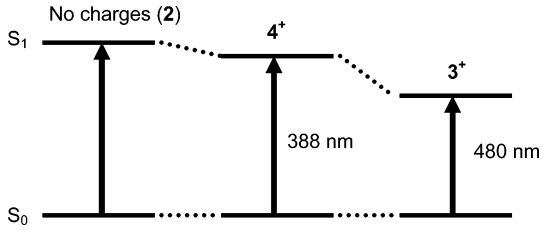

Figure 3. Schematic diagram of the shift of the energy levels for the neutral retinal Schiff base on approaching a spectator charge. To the left is the true neutral Schiff base, and to the right are the two models studied.

experiences a much larger spectral shift between the gas phase and the CH_2Cl_2 solution (+0.6 eV) than the unprotonated Schiff base retinal ($\mathbf{4}^+$) (+0.2 eV). Torii[25] theoretically examined the changes in the electronic excitation energy induced by an external electric field and found that the field-induced shifts were significantly larger for the protonated retinal Schiff base than for the neutral. Considering that such an external electric field may be present in a solvent, this result is in good agreement with the abovementioned observation.

The gas-phase value of 388 nm obtained for $\mathbf{4}^+$ is so far the best experimental gas-phase value for the intrinsic absorption maximum of the neutral retinal Schiff base. This reference value is important for comparison to calculations to optimize calculational methods. Sekharan et al.[26] recently reported a CASPT2 calculational study on the $\mathbf{3}^+$ chromophore with the $-N(CH_3)_3^+$ group reduced to $-NH_3^+$. They obtained an S_0 to S_1 energy of 484 nm, which is in perfect agreement with the experimental result at 480 nm. The S_0 to S_1 energy was also calculated for a neutral Schiff base similar to **2** but with a methyl instead of the *n*-butyl giving 357 nm. This value may be compared to the experimental absorption maximum for $\mathbf{4}^+$ at 388 nm. Whether the difference of 0.27 eV between the experimental and the theoretical result is due to small imperfections of the calculational method or is caused by a nonnegligible influence of the spectator charge is not known, but a similar high-level calculation of the S_0-S_1 excitation energy for the $\mathbf{4}^+$ molecule may resolve this question.

Great care is often needed when evaluating protein−chromophore interactions solely by comparison to solvent absorptions.[27] The gas-phase absorption maximum serves as a reference value for comparison to the UV-sensing proteins and to the functionally important photocycle intermediates with deprotonated Schiff bases. To achieve a better understanding of the spectral tuning (the so-called opsin shift) that may be induced by the protein environment, it is necessary to have such a benchmark value where solvation effects are avoided. Interestingly, metarhodopsin II experiences an absorption maximum (λ_{max} 380 nm) only slightly blue shifted relative to the gas-phase value of $\mathbf{4}^+$. In contrast, any solvent (polar or unpolar) value for λ_{max} of a true neutral model system (e.g., **2**) is blue shifted relative to that of metarhodopsin II. Thus, Becker and Freedman[22] reported the following absorption maxima of **2** in solution: 355 nm (hexane), 363 nm (benzene), 355 nm (Et_2O), 358 nm (EtOAc), 364 nm (CH_2Cl_2), 364 nm (MeOH), and 359 nm (MeCN).

Conclusion

In conclusion, we have obtained at present the best experimental gas-phase reference value for defining the opsin shift of the neutral retinal Schiff base, namely, a value of 388 nm measured for $\mathbf{4}^+$. This compound contains a neutral conjugated moiety (the chromophore part) separated from a positive

spectator charge via an ethylene bridge. It will be interesting to elucidate in the future whether we will approach experimentally the calculated absorption wavelength of 357 nm for a truly neutral chromophore by further reducing the influence of the spectator charge in suitably designed systems. Thus, both solution and gas-phase studies reveal that when a positive charge approaches the chromophore at the Schiff-base end, it results in a red shift in the absorption maximum. At the same time, we hope that our work will also stimulate high-level excitation energy calculations on $\mathbf{4}^+$. Our recent studies on protonated retinal Schiff bases show that spectral tuning in the visible region is indeed possible by environmental effects, but to reach an absorption in the UV region, it is advantageous to deprotonate the Schiff base, since deprotonation causes a blue shift of more than 200 nm. Finally, we found that the absorption maximum of the neutral retinal Schiff base is less influenced by the environment than that of the protonated retinal Schiff base.

Acknowledgment. The Lundbeck Foundation and the Velux Foundation are gratefully acknowledged for supporting this project. Moreover, we acknowledge financial support from the Danish Natural Science Research Council (grants # 2111-04-0018 and 21-03-0330).

References and Notes

(1) Spudich, J. L.; Yang, C.-S.; Jung, K.-H.; Spudich, E. N. *Annu. Rev. Cell Dev. Biol.* **2000**, *16*, 365−392.

(2) Wald, G. *Science* **1968**, *162*, 230−239.

(3) Stryer, L. *J. Biol. Chem.* **1991**, *266*, 10711−10714.

(4) Pebay-Peyroula, E.; Rummel, G.; Rosenbusch, J. P.; Landau, E. M. *Science* **1997**, *277*, 1676−1681.

(5) Palczewski, K.; Kumasaka, T.; Hori, T.; Behnke, C. A.; Motoshima, H.; Fox, B. A.; Trong, I. L.; Teller, D. C.; Okada, T.; Stenkamp, R. E.; Yamamoto, M.; Miyano, M. *Science* **2000**, *289*, 739−745.

(6) Yoshizawa, T.; Wald, G. *Nature* **1963**, *197*, 1279−1286.

(7) Neutze, R.; Pebay-Peyroula, E.; Edman, K.; Royant, A.; Navarrod, J.; Landau, E. M. *Biochim. Biophys. Acta* **2002**, *1565*, 144−167.

(8) Hunt, D. M.; Wilkie, S. E.; Bowmaker, J. K.; Poopalasundaram, S. *Cell. Mol. Life Sci.* **2001**, *58*, 1583−1598.

(9) Shi, Y.; Radlwimmer, F. B.; Yokoyama, S. *Proc. Natl. Acad. Sci. U.S.A.* **2001**, *98*, 11731−11736.

(10) Salcedo, E.; Zheng, L. J.; Phistry, M.; Bagg, E. E.; Britt, S. G. *J. Neurosci.* **2003**, *23*, 10873−10878.

(11) Zhukovsky, E. A.; Oprian, D. D. *Science* **1989**, *246*, 928−930.

(12) Sakmar, T. P.; Franke, R. R.; Khorana, H. G. *Proc. Natl. Acad. Sci. U.S.A.* **1989**, *86*, 8309−8313.

(13) Andersen, L. H.; Nielsen, I. B.; Kristensen, M. B.; El Ghazaly, M. O. A.; Haacke, S.; Nielsen, M. B.; Petersen, M. Å. *J. Am. Chem. Soc.* **2005**, *127*, 12347−12350.

(14) Nielsen, I. B.; Lammich, L.; Andersen, L. H. *Phys. Rev. Lett.* **2006**, *96*, 018304.

(15) Petersen, M. Å.; Nielsen, I. B.; Kristensen, M. B.; Kadziola, A.; Lammich, L.; Andersen, L. H.; Nielsen, M. B. *Org. Biomol. Chem.* **2006**, *4*, 1546−1554.

(16) Dawson, M. I.; Hobbs, P. D.; Kuhlmann, K.; Fung, V. A.; Helmes, C. T.; Chao, W.-R. *J. Med. Chem.* **1980**, *23*, 1013−1022.

(17) Andersen, J. U.; Hvelplund, P.; Nielsen, S. Brøndsted, Tomita, S.; Wahlgreen, H.; Møller, S. P.; Pedersen, U. V.; Forster, J. S.; Jørgensen, T. J. D. *Rev. Sci. Instrum.* **2002**, *73*, 1284−1287.

(18) Møller, S. P. *Nucl. Instrum. Methods Phys. Res., Sect. A* **1997**, *394*, 281−286.

(19) Andersen, L. H.; Heber, O.; Zajfman, D. *J. Phys. B* **2004**, *37*, R57−R88.

(20) Andersen, L. H.; Bluhme, H.; Boyé, S.; Jørgensen, T. J. D.; Krogh, H.; Nielsen, I. B.; Nielsen, S. B.; Svendsen, A. *Phys. Chem. Chem. Phys.* **2004**, *6*, 2617−2627.

(21) Frisch, M. J.; Trucks, G. W.; Schlegel, H. B.; Scuseria, G. E.; Robb, M. A.; Cheeseman, J. R.; Montgomery, J. A., Jr.; Vreven, T.; Kudin, K. N.; Burant, J. C.; Millam, J. M.; Iyengar, S. S.; Tomasi, J.; Barone, V.; Mennucci, B.; Cossi, M.; Scalmani, G.; Rega, N.; Petersson, G. A.; Nakatsuji, H.; Hada, M.; Ehara, M.; Toyota, K.; Fukuda, R.; Hasegawa, J.; Ishida, M.; Nakajima, T.; Honda, Y.; Kitao, O.; Nakai, H.; Klene, M.; Li, X.; Knox, J. E.; Hratchian, H. P.; Cross, J. B.; Adamo, C.; Jaramillo, J.; Gomperts, R.; Stratmann, R. E.; Yazyev, O.; Austin, A. J.; Cammi, R.; Pomelli, C.; Ochterski, J. W.; Ayala, P. Y.; Morokuma, K.; Voth, G. A.; Salvador, P.; Dannenberg, J. J.; Zakrzewski, V. G.; Dapprich, S.; Daniels, A. D.; Strain, M. C.; Farkas, O.; Malick, D. K.; Rabuck, A. D.; Raghavachari, K.; Foresman, J. B.; Ortiz, J. V.; Cui, Q.; Baboul, A. G.; Clifford, S.; Cioslowski, J.; Stefanov, B. B.; Liu, G.; Liashenko, A.; Piskorz, P.; Komaromi, I.; Martin, R. L.; Fox, D. J.; Keith, T.; Al-Laham, M. A.; Peng, C. Y.; Nanayakkara, A.; Challacombe, M.; Gill, P. M. W.; Johnson, B.; Chen, W.; Wong, M. W.; Gonzalez, C.; Pople, J. A. *Gaussian 03*, Revision B.03; Gaussian, Inc.: Pittsburgh, PA, 2003.

(22) Becker, R. S.; Freedman, K. *J. Am. Chem. Soc.* **1985**, *107*, 1477−1485.

(23) Mathies, R.; Stryer, L. *Proc. Natl. Acad. Sci. U.S.A.* **1976**, *73*, 2169−2173.

(24) For a similar reasoning of the electrostatic effects of external electrostatic fields on the stability of the excited states in retinal chromophores, see: (a) Cembran, A.; Bernardi, F.; Olivucci, M.; Garavelli, M. *J. Am. Chem. Soc.* **2004**, *126*, 16018−16037. (b) Cembran, A.; Bernardi, F.; Olivucci, M.; Garavelli, M. *Proc. Natl. Acad. Sci. U.S.A.* **2005**, *102*, 6255−6260.

(25) Torii, H. *J. Am. Chem. Soc.* **2002**, *124*, 9272−9277.

(26) Sekharan, S.; Weingart, O.; Buss, V. *Biophys. J.* **2006**, L07.

(27) Nielsen, S. Brøndsted; Lapierre, A.; Andersen, J. U.; Pedersen, U. V.; Tomita, S.; Andersen, L. H. *Phys. Rev. Lett.* **2001**, *87*, 228102.